Low Temperature Heat Capacity of Layered Superconductors $SrNi_2Ge_2$ and $SrPd_2Ge_2$

T. L. Hung, I. A. Chen, C. H. Huang, C. Y. Lin, C. W. Chen, Y. B. You, S. T. Jian, M. C. Yang, Y. Y. Hsu, J. C. Ho, Y. Y. Chen, et al.

Springer

Low Temperature Heat Capacity of Layered Superconductors SrNi₂Ge₂ and SrPd₂Ge₂

T.L. Hung · I.A. Chen · C.H. Huang · C.Y. Lin ·
C.W. Chen · Y.B. You · S.T. Jian · M.C. Yang ·
Y.Y. Hsu · J.C. Ho · Y.Y. Chen · H.C. Ku

Abstract Low-temperature heat capacity $C(T)$ of the weakly electron-correlated SrNi₂Ge₂ 122-layer compound undergoes a superconducting transition with onset at 1.4 K and a bulk $T_c = 0.75$ K, where heat-capacity jump ratio $\Delta C(T_c)/\gamma T_c = 0.88$–1.05. A small average superconducting energy gap E_g(ave) $= 2.21\ kT_c = 0.14$ meV is derived for this multi-gap superconductor. Similar results for isostructural SrPd₂Ge₂ include T_c(onset) = 3.5 K, bulk T_c of 2.92 K, $\Delta C(T_c)/\gamma T_c = 0.70$ and E_g(ave) $= 2.54\ kT_c = 0.64$ meV. The higher T_c onset could be associated with stoichiometric 1:2:2 grains in the polycrystalline samples. In addition, deviations of E_g/kT_c from the BCS ratio of 3.5 suggest that, just like their iron-based counterpart, these 122-layer germanides may also exhibit an unconventional, fully-opened multi-gap s-wave superconductivity.

Keywords Superconducting materials · Heat capacity · 122-layer germanide

1 Introduction

The discovery of high temperature superconductivity with transition temperatures T_c up to 55 K in strongly electron-correlated LaFeAs(O₁₋ₓFₓ) has generated a profound interest in iron-based layer systems [1].

J.C. Ho is visiting from Wichita State University, USA.

T.L. Hung · I.A. Chen · C.H. Huang · C.Y. Lin · C.W. Chen · Y.B. You · H.C. Ku (✉)
Department of Physics, National Tsing Hua University, Hsinchu 30013, Taiwan, ROC
e-mail: hcku@phys.nthu.edu.tw

S.T. Jian · M.C. Yang · Y.Y. Hsu
Department of Physics, National Taiwan Normal University, Taipei 10677, Taiwan, ROC

J.C. Ho · Y.Y. Chen
Institute of Physics, Academia Sinica, Taipei 11529, Taiwan, ROC

For the Co-doped $A(Fe_{1-x}Co_x)_2As_2$ ($A =$ Ca, Sr, Ba) 122-layer system with the $ThCr_2Si_2$-type body-centered-tetragonal (bct) structure (space group $I4/mmm$), T_c up to 22 K was observed near the antiferromagnetic spin density wave (SDW) transition of the undoped AFe_2As_2 [2–10]. Local density approximation (LDA) band calculations indicate that the $3d$ electron density of states (DOS) has a downward shift on Co-$3d^7$ bands with a stronger Co-$3d^7$-As-$4p$ hybridization. The LDA Fermi surface shows low dispersive 2D-like d bands and Co affects heavy hole-like bands at zone center, but not lighter electron-like bands around zone boundary [2–4].

For the Fe-deficient $K_{1-x}Fe_{2-y}Se_2$ 122-layer system, superconductivity up to 32 K occurs only in the vacancy-free stoichiometric KFe_2Se_2, and not in the vacancy-stabilized tetragonal superstructure $K_{0.8}Fe_{1.6}Se_2$ [11–13].

The disconnected 2D hole- and electron-pockets containing Fermi surface is believed to be the cause of an unconventional multi-gap s-wave superconductivity with possible sign-reversal between hole and electron pockets ($s_{\pm}$-wave) [14, 15].

Relevant to this study is the occurrence of superconductivity in the germanide system of SrT_2Ge_2 ($T = 3d$ or $4d$ transition metals) with a similar bct structure where $(TGe)^-$ layers are separated by Sr^{2+} layers [16–20]. T_c has been reported to be 3.04 K for $SrPd_2Ge_2$ [16], and 1.1 K for $SrNi_2Ge_2$ [18]. Considering the close resemblance in structural symmetry and mechanism of superconductivity between these iron-free compounds and the iron-based 122-layer systems, we have carried out a comprehensive calorimetric study on the superconducting- and normal-state thermal properties of $SrNi_2Ge_2$ and $SrPd_2Ge_2$ to supplement earlier preliminary heat capacity measurements.

2 Experiment

Ternary SrT_2Ge_2 samples ($T =$ Ni or Pd) were prepared by two-step arc melting under argon atmosphere. High purity Ni or Pd (>99.9 %) was first arc melted with Ge (99.9999 %) to form an intermediate compound TGe, which was then melted together with Sr (99.5 %). Extra Sr was added to compensate for the evaporation loss due to high vapor pressure at melting, thus ensuring the stoichiometric ratio of Sr:T:Ge $= 1:2:2$ to within 1 %. X-ray powder-diffraction data were collected by a Rigaku Rotaflex 18-kW rotating anode diffractometer.

Low-temperature heat capacity measurements down to 0.3 K and in applied fields up to 1 T were made in a ^{3}He cryostat using a thermal relaxation method with a RuO_2 thin-film thermometer. Additional characterizations include electrical resistance measurements down to 0.4 K by the standard four-probe method, and low-field magnetic susceptibility measurements down to 2 K by using a Quantum Design 1-T μ-metal shielded MPMS$_2$ Superconducting Quantum Interference Device (SQUID) magnetometer.

3 Results and Discussion

The as-melted polycrystalline samples show single-phase bct structure (space group $I4/mmm$) with tetragonal lattice parameters $a = 0.4160(4)$ nm, $c = 1.0187(10)$ nm

Fig. 1 Low-temperature heat capacity $C(T)$ of superconducting SrNi$_2$Ge$_2$ ($T_c = 0.75$ K) and SrPd$_2$Ge$_2$ ($T_c = 2.92$ K) (Color figure online)
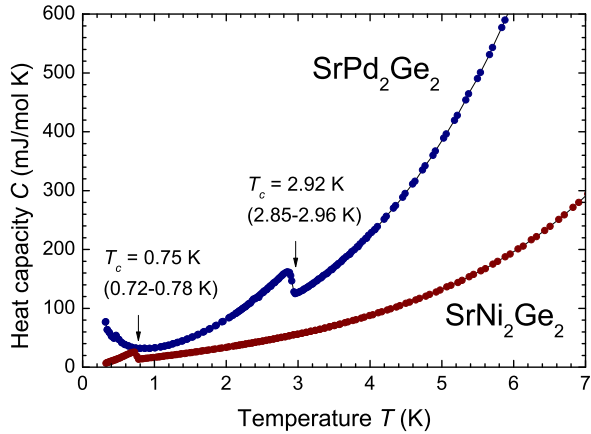
Fig. 2 Electrical resistance of SrNi$_2$Ge$_2$ indicates a T_c onset of 1.1 K. The molar magnetic susceptibility of SrPd$_2$Ge$_2$ indicates a T_c onset of 3.2 K at 10 G (Color figure online)
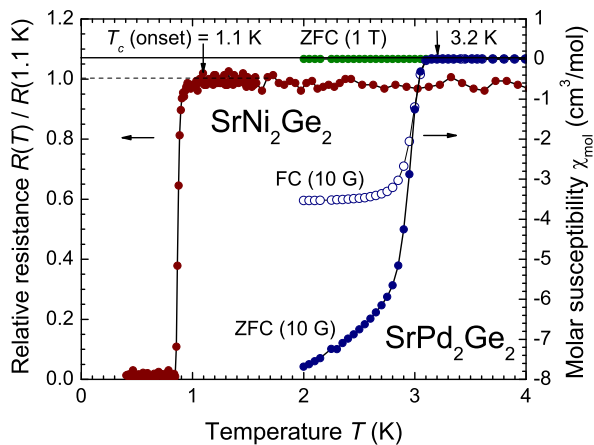
for SrNi$_2$Ge$_2$ and $a = 0.4397(4)$ nm, $c = 1.0065(10)$ nm for SrPd$_2$Ge$_2$. Their low-temperature heat capacity $C(T)$ data are shown in Fig. 1. A bulk-superconducting heat-capacity jump $\Delta C = 12.0$ mJ/mol K prevails in SrNi$_2$Ge$_2$ at the midpoint $T_c = 0.75$ K of a transition width of 0.72–0.78 K. This new specimen presents the same onset $T_c = 0.78$ K as the previous measurement [20]. For SrPd$_2$Ge$_2$, similar results yield $\Delta C = 37.1$ mJ/mol K, $T_c = 2.92$ K and a transition width of 2.85–2.96 K.

Corroborative evidence of the of the superconducting transition is given in Fig. 2. The electrical resistance of SrNi$_2$Ge$_2$ indicates a T_c onset of 1.1 K with zero-resistance T_c(zero) = 0.87 K. Due to the short-circuit nature of resistivity measurements, it is not surprising to have the higher T_c onset, which suggests that as-melted samples with nominal composition Sr$_{1-x}T_{2-y}$Ge$_2$ may contain some vacancy-free 1:2:2 stoichiometric phase [13].

For SrPd$_2$Ge$_2$, a higher T_c onset of 3.2 K was observed in 10-G low-field magnetic susceptibility measurements as shown in Fig. 2. Large zero-field-cooled (ZFC) shielding signals of -7.68 cm^3/mol at 2 K and -1.26 cm^3/mol at 3 K were observed

Fig. 3 C/T versus T^2 plot of SrNi$_2$Ge$_2$, with T_c onset around 1.4 K (Color figure online)
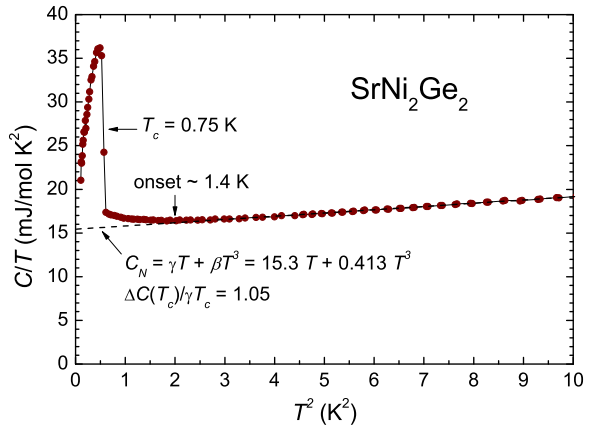
Fig. 4 $(C - \beta T^3)/\gamma T_c$ versus T/T_c plot for SrNi$_2$Ge$_2$, with a superconducting gap $E_g(\text{ave}) = 0.14$ meV (Color figure online)
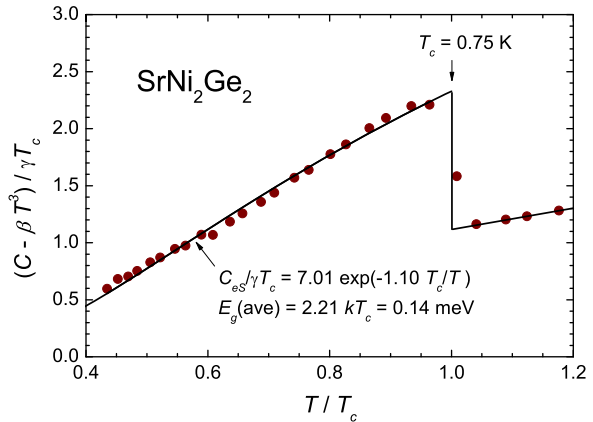
with field-cooled (FC) Meissner signals of -3.53 cm^3/mol at 2 K and -1.26 cm^3/mol at 3 K. The T_c of 3.2 K is the highest T_c reported so far for SrPd$_2$Ge$_2$. Again, this higher T_c may be associated with some stoichiometric 1:2:2 grains in the polycrystalline samples. No T_c above 2 K was observed in SrPd$_2$Ge$_2$ at a 1-T applied field.

A C/T versus T^2 plot for SrNi$_2$Ge$_2$ with $T_c = 0.75$ K is shown in Fig. 3. Above T_c, the normal-state heat capacity from 1.4 K to 3.2 K can be fitted with the formula $C_N(T) = C_{eN} + C_{Debye} = \gamma T + \beta T^3$, with an electronic term coefficient $\gamma = 15.3$ mJ/mol K^2 and a Debye temperature $\theta_D = 287$ K from $\beta = 0.413$ mJ/mol K^4. A slightly upturn deviation from linearity starts around 1.4 K, which is even higher than the resistivity T_c onset of 1.1 K. Again, the higher T_c may be due to some 1:2:2 stoichiometric phase in the polycrystalline sample. The derived superconducting heat-capacity jump ratio $\Delta C(T_c)/\gamma T_c$ of 1.05 is lower than the BCS value of 1.43.

A $(C - \beta T^3)/\gamma T_c$ versus T/T_c plot for SrNi$_2$Ge$_2$ is shown in Fig. 4. Below $T_c = 0.75$ K, the superconducting electronic heat capacity contribution $C_{eS}(T) = C_{eS} - \beta T^3$ can be roughly fitted with a simple exponential formula $C_{eS}/\gamma T_c =$

Fig. 5 Low-temperature heat capacity (*inset*) and C/T versus T^2 plot for SrNi$_2$Ge$_2$ (*Sample II*) in applied fields $B_a = 0$, 80 G, and 1 T. *In the inset*, an onset at 0.57 K in 1-T field (*vertical arrow*), a midpoint at 0.62 K in 80-G field (*diagonal arrow*), and a midpoint at 0.75 K in zero field (*horizontal arrow*) are shown (Color figure online)
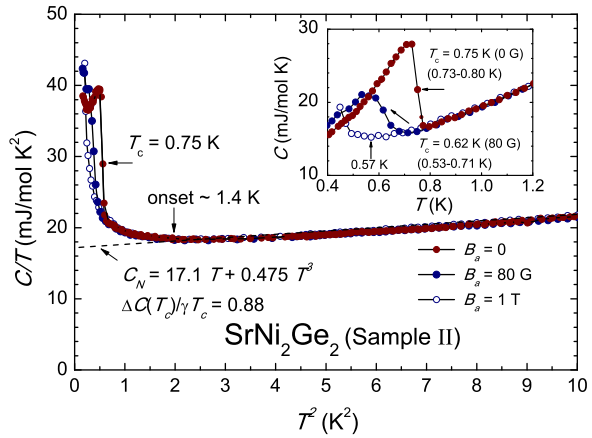
$7.01 \exp(-1.10 T_c/T)$ which suggests an average superconducting energy gap $E_g(\text{ave}) = 2.21 \, kT_c = 0.14$ meV for this multi-gap s-wave-like superconductor. The ratio $E_g(\text{ave})/kT_c$ is lower than the BCS value of $E_g(0)/kT_c = 3.5$.

A band-structure calculation for SrT_2Ge$_2$ ($T =$ Ni, Pd) suggests that, with 30 valence electrons per formula unit, as compared to 28 valence electrons for the quasi-2D-like BaFe$_2$As$_2$, the Fermi level shifts up into the upper manifold of T-nd/Ge-4p hybridized bands where, in addition to d_{xy} and $d_{x^2-y^2}$ bands, large contributions exist from d_{xz}, d_{yz}, and d_{z^2} bands. As a result, the Fermi surface is transformed into a multi-sheet 3D-like structure [17].

The deviations of $\Delta C(T_c)/\gamma T_c$ and E_g/kT_c from the BCS values suggest that SrNi$_2$Ge2 is of an unconventional multi-gap s-wave nature and similar to that of iron-based superconductors [14, 15]. The lower superconducting transition temperature of this electron-overdoped material in the weakly electron-correlated Fermi liquid regime is the direct result of more dispersive 3D-like Fermi surface. The observed γ value of 15.3 mJ/mol K^2 is higher than 7.85 mJ/mol K^2 calculated from the free electron model and indicates the effect of electron-correlation for this multi-gap superconductor.

To check the validity of the fit and the field-dependent superconducting- and normal-state properties, $C(B_a)/T$ versus T^2 of another SrNi$_2$Ge$_2$ (Sample II) in applied fields $B_a = 0$, 80 G, and 1 T are shown in Fig. 5. Identical midpoint T_c of 0.75 K (inset) with transition width 0.73–0.80 K was observed at zero field, and T_c decreases to 0.62 K with transition width 0.53–0.71 K in 80 G. Heat-capacity jump onset at 0.57 K was clearly observed in 1-T field with an extrapolated upper critical field H$_{c2}$(0 K) = 5 T.

The normal-state heat capacity $C_N(B_a)$ above 1.4 K in three different fields can all be fitted with $C_N(T) = C_{eN} + C_{Debye} = \gamma T + \beta T^3$ with a slightly larger but field-independent $\gamma = 17.1$ mJ/mol K^2 and a Debye temperature $\theta_D = 274$ K from $\beta = 0.475$ mJ/mol K^4. Again, an upturn deviation from linearity indicates a T_c onset around 1.4 K. The superconducting heat-capacity jump ratio $\Delta C(T_c)/\gamma T_c$ is 0.88. Since both samples show an 122 single phase, the slightly different values observed

Fig. 6 C/T versus T^2 for SrPd$_2$Ge$_2$, with T_c onset around 3.5 K (Color figure online)
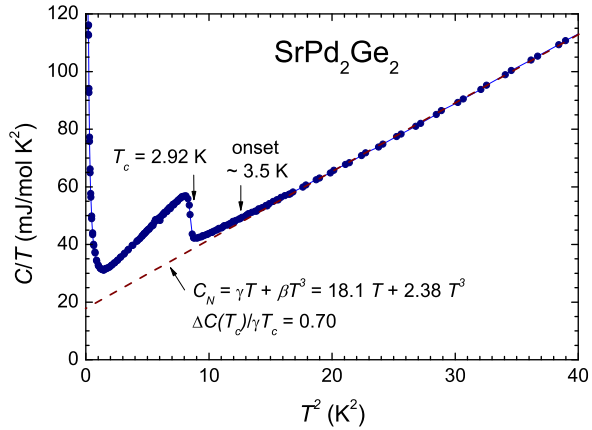
Fig. 7 $(C - \beta T^3)/\gamma T_c$ versus T/T_c for SrPd$_2$Ge$_2$, with a superconducting gap E_g(ave) = 0.64 meV (Color figure online)
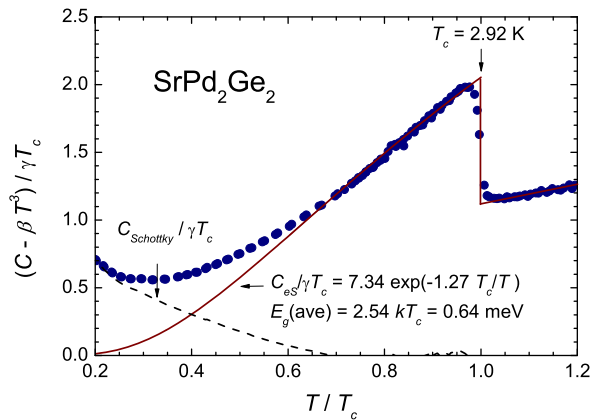
may be due to a slight composition variation of Sr$_{1-x}$Ni$_{2-y}$Ge$_2$ in the arc melting processes.

A C/T versus T^2 plot for SrPd$_2$Ge$_2$ having the higher $T_c = 2.92$ K is shown in Fig. 6. Above T_c, the normal-state heat capacity from 3.5 K to 6.3 K can also be fitted with the formula $C_N(T) = \gamma T + \beta T^3$, but with a larger normal-state electronic coefficient $\gamma = 18.1$ mJ/mol K^2 and a lower Debye temperature $\theta_D = 160$ K from $\beta = 2.38$ mJ/mol K^4. The upturn deviation from linearity indicates a T_c onset around 3.5 K which is higher than 3.2 K from the magnetic susceptibility data. This supports our speculation that stoichiometric ratio of 1:2:2 is crucial for an elevated T_c.

The superconducting specific-heat jump ratio $\Delta C(T_c)/\gamma T_c$ of 0.70 is even lower than 0.88–1.05 observed for SrNi$_2$Ge$_2$, further indicating an unconventional nature of s-wave superconductivity in these compounds.

A $(C - \beta T^3)/\gamma T_c$ versus T/T_c plot for SrPd$_2$Ge$_2$ is shown in Fig. 7. At low temperatures, a Schottky-type contribution is observed and the superconducting-state heat capacity, after having the lattice term substracted, $C_S - \beta T^3 = C_{eS} + C_{Schottky}$. However, the Schottky-type contribution decreases rapidly with increasing tempera-

ture and becomes totally negligible for $T > 1.5$ K. As a result, the superconducting electronic heat capacity C_{eS} above 1.5 K can be roughly fitted with exponential formula $C_{eS}/\gamma T_c = 7.34\exp(-1.27 T_c/T)$ which corresponds to a larger average superconducting energy gap $E_g(\text{ave}) = 2.54\,kT_c = 0.64$ meV.

The additional contribution to the observed heat capacity below 1.5 K increases with decreasing temperature, resembling roughly to the high-temperature tail of a nuclear Schottky term. Without any magnetic ordering of electronic moments to induce a magnetic hyperfine field here, the anomaly is presumably a nuclear quadrupole term, which is caused by the alignment of nuclear quadrupole moment in the electric field gradient of the crystal. Its magnitude relies on the non-zero quadrupole moment and a large electric field gradient at nucleus. Palladium is the most likely source, since it has an isotope, ^{105}Pd, with higher natural abundance (22.3 %) as well as a larger nuclear quadrupole moment ($+6.6 \times 10^{-29}$ m^2) than nickel (^{61}Ni, 1.14 %, $+1.62 \times 10^{-29}$ m^2), strontium (^{87}Sr, 7.0 %, $+3.35 \times 10^{-29}$ m^2) or germanium (^{73}Ge, 7.73 %, -1.73×10^{-29} m^2). Indeed, no similar anomaly was observed in SrNi$_2$Ge$_2$. The highly anisotropic layered structure of SrPd$_2$Ge$_2$ must be responsible for the large electric field gradient.

The observed γ value of 18.1 mJ/mol K^2 is higher than that of SrNi$_2$Ge$_2$ and much higher than 6.84 mJ/mol K^2 calculated from the free electron model. Previously reported single crystal heat-capacity data with a lower T_c of 2.67 K in a narrow temperature measurement range from 2 to 3.5 K may be unreliable [19]. Low T_c suggests that the flux-grown single crystal may not of the stoichiometric 1:2:2 composition. The curve-fitting below heat capacity upturn of 3.5 K had led to an incorrect $\Delta C(T_c)/\gamma T_c$ value of 2.1 instead of 0.70 revealed in this report.

4 Conclusion

Low-temperature heat capacity $C(T)$ of multi-gap SrNi$_2$Ge$_2$ with $T_c = 0.75$ K shows a heat-capacity jump ratio $\Delta C(T_c)/\gamma T_c = 0.88$–1.05 and an average superconducting energy gap $E_g(\text{ave}) = 2.21\,kT_c = 0.14$ meV. For SrPd$_2$Ge$_2$ with $T_c = 2.92$ K, the jump ratio is $\Delta C(T_c)/\gamma T_c = 0.70$ and $E_g(\text{ave}) = 2.54\,kT_c = 0.64$ meV. An observed higher T_c onset is likely associated with some stoichiometric 1:2:2 grains in the sample. The deviation of E_g/kT_c from the BCS ratio of 3.5 suggests that these 122-layer germanide compounds may exhibit s-wave multi-band superconducting gaps and be of an unconventional s-wave nature as proposed for iron-based superconductors.

References

1. Y. Kamihara, T. Watanabe, M. Hirano, H. Hosono, J. Am. Chem. Soc. **130**, 3296 (2008)
2. A.S. Sefat, R. Jin, M.A. McGuire, B.C. Sales, D.J. Singh, D. Mandrus, Phys. Rev. Lett. **101**, 117004 (2008)
3. D.J. Singh, Phys. Rev. B **78**, 094511 (2008)
4. E. Aktürk, S. Ciraci, Phys. Rev. B **79**, 184523 (2009)

5. T.-M. Chuang, M.P. Allan, J. Lee, Y. Xie, N. Ni, S.L. Bud'ko, G.S. Boebinger, P.C. Canfield, J.C. Davis, Science **327**, 181 (2010)
6. N. Ni, S. Nandi, A. Kreyssig, A.I. Goldman, E.D. Mun, S.L. Bud'ko, P.C. Canfield, Phys. Rev. B **78**, 014523 (2008)
7. H. Hosono, Physica C **469**, 314 (2009)
8. A.I. Goldman, D.N. Argyriou, B. Ouladdiaf, T. Chatterji, A. Kreyssig, S. Nandi, N. Ni, S.L. Bud'ko, P.C. Canfield, R.J. McQueeney, Phys. Rev. B **78**, 100506 (2008)
9. S.-H. Baek, N.J. Curro, T. Klimczuk, E.D. Bauer, F. Ronning, J.D. Thompson, Phys. Rev. B **79**, 052504 (2009)
10. J.-H. Chu, J.G. Analytis, C. Kucharczyk, I.R. Fisher, Phys. Rev. B **79**, 014506 (2009)
11. J. Guo, S. Jin, G. Wang, S. Wang, K. Zhu, T. Zhou, M. He, X. Chen, Phys. Rev. B **82**, 180520(R) (2010)
12. A.F. Wang, J.J. Ying, Y.J. Yan, R.H. Liu, X.G. Luo, Z.Y. Li, X.F. Wang, M. Zhang, G.J. Ye, P. Cheng, Z.J. Xiang, X.H. Chen, Phys. Rev. B **83**, 060512(R) (2011)
13. W. Li, H. Ding, P. Deng, K. Chang, C. Song, K. He, L. Wang, X. Ma, J.-P. Hu, X. Chen, Q.-K. Xue, Nat. Phys. **8**, 126 (2012)
14. I.I. Mazin, D.J. Singh, M.D. Johannes, M.H. Du, Phys. Rev. Lett. **101**, 057003 (2008), and reference cited therein
15. T. Hanaguri, S. Niitaka, K. Kuroki, H. Takagi, Science **328**, 474 (2010), and reference cited therein
16. H. Fujii, A. Sato, Phys. Rev. B **79**, 224522 (2009)
17. I.R. Shein, A.L. Ivanovskii, Physica B **405**, 3213 (2010)
18. C.D. Yang, H.C. Hsu, W.Y. Tseng, H.C. Chen, H.C. Ku, M.N. Ou, Y.Y. Chen, Y.Y. Hsu, J. Phys. Conf. Ser. **273**, 012089 (2011)
19. N.H. Sung, J.-S. Rhyee, B.K. Cho, Phys. Rev. B **83**, 094511 (2011)
20. J.W. Wang, I.A. Chen, T.L. Huang, Y.B. You, H.C. Ku, Y.Y. Hsu, J.C. Ho, Y.Y. Chen, Phys. Rev. B **85**, 024538 (2012)